Advanced sensing materials based on molecularly imprinted polymers towards developing point-of-care diagnostics devices

Anna Kidakova, Jekaterina Reut, Roman Boroznjak, Andres Öpik, and Vitali Syritski[*]

Department of Materials and Environmental Technology, Tallinn University of Technology, Ehitajate tee 5, 19086 Tallinn, Estonia

Abstract. Today there is growing interest in the replacement of biological receptors in biosensing systems including point-of-care (PoC) diagnostics devices due to their high price and short shelf life. Molecularly imprinted polymers (MIPs), which are wholly synthetic materials with antibody-like ability to bind and discriminate between molecules, demonstrate improved stability and reduced fabrication cost as compared with biological receptors. Here we report, for the first time, a MIP-based synthetic receptor capable of selective binding of a clinically relevant protein – the brain-derived neurotrophic factor (BDNF). The BDNF-MIP was generated by surface-initiated controlled/living radical photopolymerization directly on a screen-printed electrode (SPE). The resulting BDNF-MIP/SPE electrochemical sensor could detect BDNF down to 6 pg/mL in the presence of the interfering HSA protein and was capable of discriminating BDNF among its structural analogues, i.e. neurotropic factors CDNF and MANF. We believe that the presented approach for the preparation of a neurotrophic factor-selective sensor could be a promising route towards the development of innovative PoC diagnostics devices for the early-stage diagnostics and/or monitoring the therapy of neurological diseases.

List of main abbreviations

BDNF	Brain-derived neurotrophic factor	MANF	Mesencephalic astrocyte-derived neurotrophic factor
BDNF-MIP/SPE	SPE modified by MIP film with molecular imprints of BDNF	mCD48	Mouse recombinant cluster of differentiation 48
CDNF	Cerebral dopamine neurotrophic factor	MIP	Molecularly imprinted polymer
C/LR	Controlled/living radical	NF	Neurotrophic factor
CV	Cycling voltammetry	NIP	Non-imprinted polymer
DPV	Differential pulse voltammetry	PBS	Phosphate buffer saline
EIS	Electrochemical impedance spectroscopy	PoC	Point-of-care
HSA	Human serum albumin	SPE	Screen-printed electrode
IF	Imprinting factor	WE	Working electrode
LOD	Limit of detection		
LOQ	Limit of quantitation		

[*] Corresponding author, vitali.syritski@taltech.ee

1. INTRODUCTION

Nowadays, healthcare is facing an increasing demand for fast and reliable analytical methods suitable for achieving appropriate sensitivity and selectivity with low limit of detection (LOD) while being low-cost, portable, and capable of in situ real-time monitoring.

The occurrence and use of point-of-care (PoC) devices have steadily increased in Europe [1] as well as globally for facilitating rapid testing in medical diagnostics, and thus clinical decisions [2,3]. Most of the current biosensing systems including PoC devices utilize labile biological recognition elements that offer high selectivity towards a target analyte, but limit the shelf life of the device and increase cost and analysis time. Growing interest in the replacement of biological receptors with wholly synthetic analogues such as molecularly imprinted polymers (MIPs) has made a substantial contribution to the expansion of the field [4,5]. Molecular imprinting is one of the state-of-the-art techniques to generate MIPs – materials with antibody-like ability to bind and discriminate between molecules [6]. The technique can be defined as the process of template-induced formation of specific molecular recognition sites in a polymer matrix. The main benefits of MIPs are related to their synthetic nature, i.e. excellent chemical and thermal stability coupled with their reproducible and cost-effective fabrication. MIPs have been shown to be a promising alternative to natural receptors in biosensors [7–10].

The sensors based on electrochemical transduction mechanisms seem to be prospective for diagnostics purposes since they combine real-time monitoring of an analyte binding event, simplicity in handling, and sufficient sensitivity at reduced cost [11,12]. Furthermore, screen-printed electrode (SPE) sensors, being fully compatible with large-scale fabrication and multiplexing technologies and the ease in their integration with microfluidic systems, represent an ideal starting point to realize low cost and portable sensing platforms suitable for PoC devices [13]. Therefore, robust interfacing of a MIP film with a SPE provides a considerable option to build a cost-effective but reliable PoC device [14,15].

In clinical diagnostics, the research aimed at the discovery and detection of biomarkers of human diseases, especially neurological and mental disorders, has become of great demand due to the increase in the prevalence of these diseases over the last decades and the need for early stage diagnosis [16]. For example, neurotrophic factor (NF) proteins, which are a family of proteins secreted from neurons and neuron-supporting cells, were found to be associated with a number of neurological and mental diseases [17–20]. There is a large number of publications associating brain-derived neurotrophic factor

(BDNF) levels with various conditions affecting brain functioning, including depression and neurodegeneration (Alzheimer's and Parkinson's diseases) [21–23]. Therefore, BDNF can be considered as a potential biomarker for the pre-symptomatic diagnostics of these diseases or for monitoring therapies.

The application of MIP-based sensors for diagnostics has been extensively studied. Thus, the detection of cancer biomarkers (such as prostate specific antigen [24], epithelial ovarian cancer antigen-125 [25], carcinoembryonic antigen [26]), and cardiovascular disease biomarkers (myoglobin [27,28] and cardiac troponin T [29]) by MIP-modified sensors has been reported. In addition, MIP receptors for selective extraction of an Alzheimer's disease biomarker, α-Amyloid peptides, has been studied by Sellergren's group [30]. Although the selective recognition of a growth factor family protein, vascular endothelial growth factor, by hybrid MIP nanoparticles as well as by MIP thin layer on surface plasmon resonance (SPR) and screen-printed electrodes (SPEs) has been reported [31–33], to the best of our knowledge, there are no reports on the MIP designed for the recognition of NF proteins.

When synthesizing a MIP for sensing macromolecules such as proteins, it is essential that the synthesis strategy prevent the entrapment of the protein in the polymer matrix during the polymerization process and lead to a robust interfacing of the MIP with the surface of a sensor, i.e. to an efficient transduction of the binding event of this macromolecular analyte by the MIP into useful analytical signals. To address the issues, the implementing of surface-initiated controlled/living radical (C/LR) polymerization was shown to be a prospective solution [34,35]. The method of surface-initiated polymerization allows the formation of covalent bonding between the polymer film and the surface, which ensures a perfect interfacing between the MIP recognition layer and a sensor transducer. Moreover, the C/LR polymerization offers the capability of the film thickness control, uniform coating of surface, control over composition, and high density of grafting [36]. To perform surface initiated C/LR photopolymerization, an initiator, also called iniferter (initiator–transfer agent–terminator), was attached to a sensor surface using different techniques by Ahmad et al. [37].

In the present work, for the first time the MIP-based sensor for the detection of BDNF was prepared on a SPE by C/LR photopolymerization initiated from the surface. The main analytical characteristics of the BDNF-MIP/SPE sensor, such as its limit of detection (LOD) and limit of quantification (LOQ), were determined. The BDNF-MIP/SPE sensor was studied in terms of its recognition capability and selectivity towards

the target protein through the analysis of the responses of the BDNF-MIP-modified SPE sensors to the interaction of the target (BDNF) and interfering (cerebral dopamine neurotrophic factor (CDNF), mesencephalic astrocyte-derived neurotrophic factor (MANF), mouse recombinant cluster of differentiation 48 (mCD48)) proteins.

2. EXPERIMENTAL

2.1. Chemicals and materials

3,5-Dichlorophenyl diazonium tetrafluoroborate (3,5-DClPDT), sodium diethyldithiocarbamate (Na-DEDTC), acetonitrile (ACN), (3-glycidyloxypropyl)trimethoxysilane (3-GPS), N,N′-methylenebis(acrylamide) (BAA), diethyl-aminoethyl methacrylate (DEAEM), and human serum albumin (HSA, 66.5 kDa) were obtained from Sigma-Aldrich. Tetrabutylammonium tetrafluoroborate (Bu$_4$NBF$_4$, 99.0%,) was obtained from Fluka. Human recombinant BDNF (13.5 kDa, pI 9.43), human re-combinant CDNF (18.5 kDa, pI 7.68), human recombinant MANF, (18.1 kDa, pI 8.55), and mCD48 antigen (cluster of differentiation 48, 22.2 kDa, pI 9.36) were provided by Icosagen AS (Tartu, Estonia). Ultrapure water (resistivity 18.2 MΩ·cm, Millipore, USA) was used for the preparation of all aqueous solutions. Phosphate buffered saline (PBS) solution (0.01 M, pH 7.4) was used to prepare analyte solutions. The screen-printed

electrodes (SPEs) were obtained from BVT Technologies a.s. (Praha, Czech Republic). The SPEs (catalogue #AC1.W1.R2) include a gold working electrode (WE) (1 mm diameter), an AgCl covered silver reference electrode, and a gold counter electrode.

2.2. Synthesis of BDNF-MIP films

The BDNF-MIP films were synthesized directly on the WE of the SPE using the following main stages (Fig. 1): (a) functionalization of SPE with 3,5-DClPD, (b) grafting of the iniferter to 3,5-DClPD, (c) coating of the SPE with the solution containing a mixture of the functional (DEAEM) and crosslinking (BAA) monomers and the target protein (BDNF), (d) photopolymerization of the monomers under UV-irradiation, and (e) removing BDNF from the polymer to form BDNF-MIP on the surface of the SPE.

The WE of the SPE was cleaned electrochemically by placing a drop of 0.1 M H$_2$SO$_4$ solution on it and cycling the potential from 0.1 to 1.15 V at a scan rate of 100 mV/s for 15 cycles. The modification of the WE with the 3,5-DClP layer was performed electrochemically applying an ACN solution containing 1 mM 3,5-DClPDT and 0.1 M Bu$_4$NBF$_4$ and cycling the potential of the WE between the –0.1 V and 0.5 V vs Ag/AgCl/KCl electrode at a rate of 50 mV/s. The modified surface was washed with tetrahydrofuran (THF) and ultrapure water to
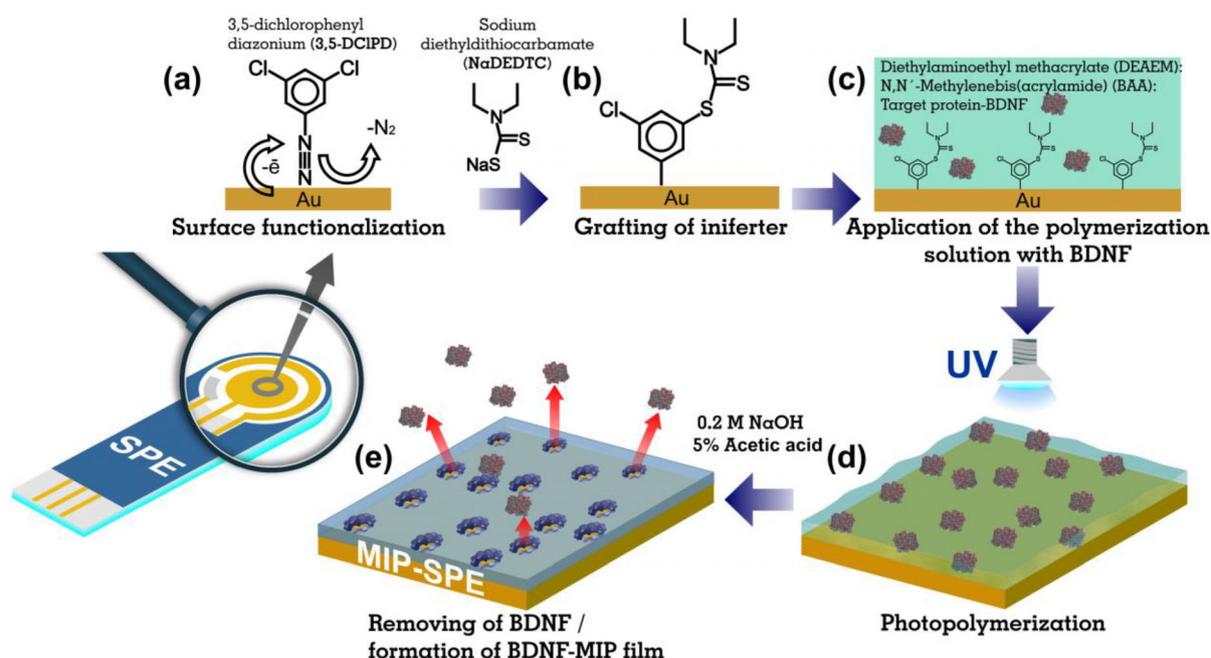

Fig. 1. Fabrication of the BDNF-MIP/SPE sensor.

remove the physisorbed loosely bound layers of a 3,5-DClP [38] and dried under a nitrogen flow. The resulting SPE sensor with a 3,5-DClP layer grafted on the WE was immersed in ethanolic solution of 2 mM Na-DEDTC and vortexed (600 rpm) overnight at room temperature in the dark. Finally, the SPE was thoroughly rinsed with ethanol and ultrapure water and dried with a nitrogen flow.

The charge transfer blocking behaviour of the 3,5-DClP layer was investigated by electrochemical impedance spectroscopy (EIS) and cyclic voltammetry (CV). The EIS and CV were conducted in 1 M KCl solution containing a 4 mM redox probe $K_3[Fe(CN)_6]/K_4[Fe(CN)_6]$ by an electrochemical workstation (Reference 600, Gamry Instruments, USA). The CV was performed scanning the potential between 0 and 0.5 V at a scan rate of 50 mV/s. The EIS was performed in the frequency range between 100 kHz and 0.1 Hz at open circuit potential with AC amplitude of 10 mV. Every CV and EIS was repeated 3 times. The EIS spectra were fitted to an equivalent electrical circuit using Echem Analyst software (Gamry Instruments, USA). The BDNF-MIP film on the DEDTC-modified WE of the SPE was generated by C/LR photopolymerization by using UV-irradiation.

The prepolymerization solution was prepared by mixing 12.5 μg/mL BDNF, 2.5 mM functional monomer, DEAEM, and 15 mM cross-linking monomer, BAA, in 0.05 M PBS. The prepolymerization solution (10 μL) was dropped onto the DEDTC-modified SPE sensor and left for 30 min. Then the SPE was covered by a mask with a hole 20% larger than the diameter of the WE and irradiated under UV light (500 W/m^2, 365 nm) during 30 min at room temperature. The optimum polymerization time was determined by comparing the normalized signals of the sensors after polymerization for 15, 30, and 45 min. The normalized signals were determined during incubation in 5 ng/mL BDNF solution in PBS. After photopolymerization the mask was removed and the SPE sensor was alternately immersed in aqueous solution of 0.2 M NaOH and 5% acetic acid and vortexed (600 rpm) for 30 min to remove the protein from the polymer matrix. The resulting BDNF-MIP/SPE sensor was washed with Milli-Q water and dried under nitrogen flow. The reference non-imprinted polymer (NIP) film was produced in the same way except that the prepolymerization solution was prepared without the addition of BDNF. The surface morphology of the BDNF-MIP and NIP films was characterized by high-resolution scanning electron microscope (HR-SEM Zeiss Merlin) equipped with an In-Lens SE detector for topographic imaging. Measurements were made at an operating voltage of 2.00 kV.

2.3. Rebinding, reusability, and selectivity studies of the BDNF-MIP/SPE sensor

The binding affinity and selectivity of the BDNF-MIP/SPE toward the target analyte BDNF were determined by means of differential pulse voltammetry (DPV). Measurements were performed in the 1 M KCl solution containing a 4 mM redox probe $K_3[Fe(CN)_6]/K_4[Fe(CN)_6]$. The DPV was conducted in the range 0–0.4 V with the pulse amplitude of 0.025 V, pulse time of 0.05 s, and step potential of 0.005 V. The DPV was performed after 30 min incubation of BDNF-MIP- and NIP-modified SPE sensors in solutions with increasing concentrations of the analyte (from 0.1 to 100 ng/mL of BDNF in PBS solution). After that, the unbound protein was removed by washing twice in PBS vortexed (600 rpm) for 5 min. The optimal incubation time was determined by incubating the BDNF-MIP/SPE sensor in the BDNF solution (2 ng/mL) for various times (5, 10, 15, 20, 30, 40, 60 min). The binding affinity of the BDNF-MIP films toward the target was measured by means of DPV. The DPV curves were recorded after the incubation of BDNF-MIP- and NIP-modified SPEs in solutions with increasing concentrations of the analyte (from 0.1 to 100 ng/mL of BDNF in PBS). The response signals of the BDNF-MIP/SPE were its normalized DPV current peaks, B_n, calculated according to Eq. (1):

$$B_n = \frac{I_0 - I_c}{I_0}, \qquad (1)$$

where I_0 is DPV current peak measured after the incubation of the SPE in blank PBS solution, I_C is the DPV current peak measured after the incubation the SPE in PBS containing a particular concentration (C) of BDNF.

The binding isotherms were generated using B_n values. The values of the dissociation constant (K_d) and the maximum binding response at saturation (B_{max}) were derived from fitting the binding isotherm to Langmuir adsorption models (Eq. 2):

$$B = \frac{B_{max} C}{K_d + C}. \qquad (2)$$

The reusability of the BDNF-MIP/SPE sensor was tested by measuring its responses after the regeneration procedure and repeated incubation in BDNF solution (2 ng/mL). The regeneration procedure was performed in the same way as the procedure for the removal of the protein from the polymer matrix employed after the synthesis of the BDNF-MIP film. The selectivity of the BDNF-MIP/SPE sensor was assessed by comparing the

responses of the BDNF-MIP/SPE sensor towards BDNF with those of the interfering proteins CDNF, MANF, and mCD48. The selectivity test was conducted at different concentrations of the proteins in the presence of 0.8 mg/mL HSA.

3. RESULTS AND DISCUSSION

3.1. Preparation of BDNF-MIP films

In this study the BDNF-MIP films were prepared by the surface-initiated C/LR polymerization technique directly on the WE of the SPE. First, the WE of the SPE was modified by a 3,5-dichlorophenyl (3,5-DClP) layer using the electrochemical reduction of the corresponding aryldiazonium salt, 3,5-DClPDT. This is a well-known method and widely used to modify metal surfaces by organic molecules providing the formation of a stable molecular layer as a result of covalent bonding of the aryl radical to the metal surface [39,40]. Figure 2 illustrates CV of the electrodeposition process of 3,5-DClP. The first cycle reveals well-defined reduction peaks, which can be attributed to the electrochemical reduction of 3.5-DClPDT to its corresponding radicals. The reduction peaks disappear during the second cycle, which corresponds to the formation of a blocking layer preventing further access of the diazonium species to the electrode surface [41].

The success of the modification of the WE by 3,5 DClP was confirmed by CV and EIS recorded in the presence of a $Fe(CN)_6^{3-/4-}$ redox pair. Figure 3a shows that the intensity of the pair of the current peaks associated with the redox activity of $Fe(CN)_6^{3-/4-}$ and defined well on the bare gold electrode, greatly diminished after the grafting of the diazonium salt on the gold electrode. This confirms the insulating nature of the deposited
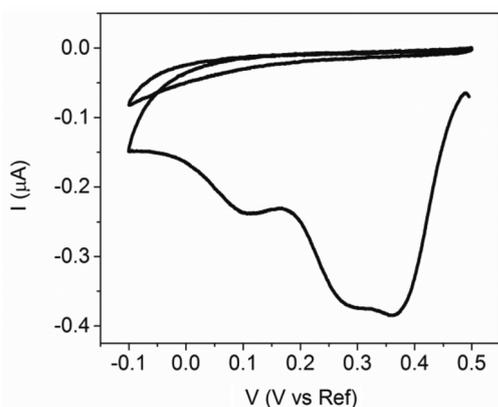
Fig. 2. Cyclic voltammograms recorded on the bare gold electrodes in the acetonitrile solution containing 0.1 M Bu_4NBF_4 and 1 mM 3,5-DClPDT; scan rate 50 mV/s.
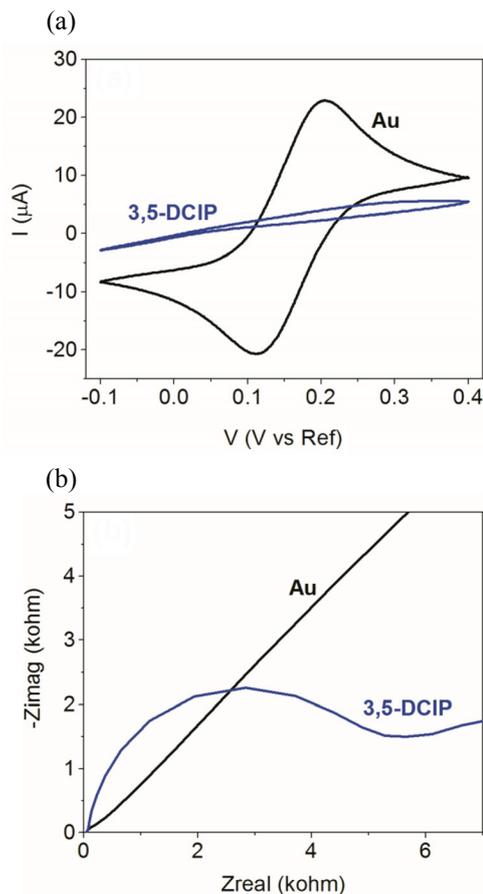
Fig. 3. Cyclic voltammogram at the scan rate of 50 mV/s (a) and the Nyquist plot for the bare gold (Au) and 3,5-DClP-modified gold (b).

organic monolayers. The charge transfer resistance, as estimated from the width of the semicircle in the Nyquist plot (Fig. 3b), increased from 68 Ω/cm^2 (the bare gold electrode) to 2.3 kΩ/cm^2 (after modification by the 3.5-DClP layer). The increase in the charge transfer resistance is a direct consequence of the partial passivation of the bare gold electrode, which reduces the ability of the redox probe to access its surface. The attachment of the iniferter DEDTC to the 3,5-DClP-modified surfaces by electrophilic substitution was discussed in detail in our previous work [35], where the successful functionalization of the gold electrode by a DEDTC layer was additionally confirmed by X-ray photoelectron spectroscopy data.

To synthesize a protein-selective MIP film, it is essential to prevent the entrapment of protein in the polymer matrix during the polymerization process. Therefore, in order to avoid the overgrowing of the polymer around the BDNF molecules, the thickness of the photopolymerized polymer film was controlled by the UV exposure time. The optimal exposure time was
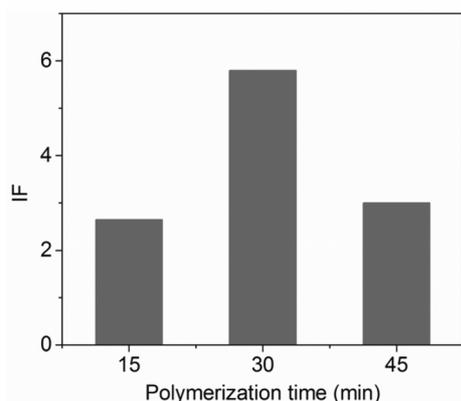
Fig. 4. Calculated *IF* values for the BDNF-MIP/SPE sensor prepared at different polymerization times.

Fig. 5. Normalized response of a BDNF-MIP/SPE sensor as a function of the incubation time in 5 ng/mL BDNF solution.

determined by calculating the imprinting factor (*IF*) (Eq. 3), which characterizes the relative adsorption capacity of MIP.
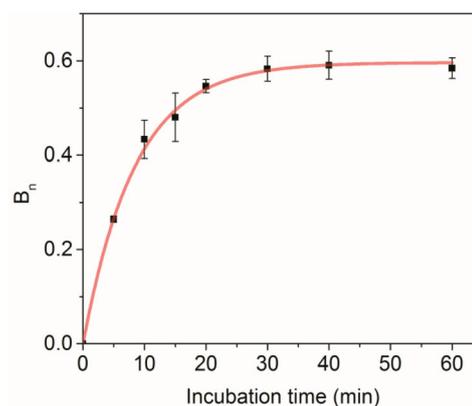
$$IF = \frac{B_n MIP}{B_n NIP} , \qquad (3)$$

where $B_n MIP$ and $B_n NIP$ are normalized signals after protein adsorption on MIP and NIP, respectively; *IF* reflects the quality of the imprinting effect, as a larger value of *IF* represents the availability of more binding sites with high affinity in the resulting polymer. As can be seen in Fig. 4, the BDNF-MIP shows a higher *IF* value after 30 min of photopolymerization. The UV irradiation of 500 W/m^2 was chosen as the optimal intensity that does not cause significant damage to the protein structure within 30 min of exposure [35].
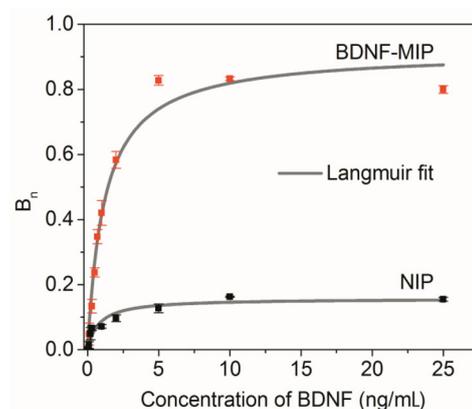
3.2. Analytical performance of a BDNF-MIP/SPE sensor

The binding affinity of the BDNF-MIP/SPE toward the target analyte BDNF was determined by means of DPV recorded after the incubation of the sensor in the solution with an increased concentration of the analyte. Firstly, in order to select the optimal binding conditions, the relationship between the sensor signal B_n and the incubation time in the range of 5–60 min was studied. The current increased rapidly within the first 20 min of incubation and reached the saturation value after 30 min (Fig. 5), indicating that the adsorption equilibrium was reached. Thus, the optimal incubation time of 30 min was chosen for the rebinding study.

The B_n values calculated from Eq. (1) were used to plot the binding isotherms (Fig. 6). The BDNF-MIP/SPE sensor showed a hyperbolic response as a function of the BDNF concentrations. To describe the equilibrium


Fig. 6. Binding isotherms of BDNF to the BDNF-MIP- and NIP-modified SPE sensor.

binding events happening on the sensor surface, the Langmuir adsorption model was used in this study. The Langmuir binding model was previously successfully applied to fit the adsorption isotherm of MIPs by other authors [27,29,42]. According to the model, when all binding sites are occupied by molecules, no further adsorption will occur on the surface and the saturation response (B_{max}) will be obtained. The fitting results showed that BDNF-MIP bound the target protein, BDNF, with the dissociation constant K_d of 1.12 ng/mL and had an about 5.8 times higher binding capacity than NIP as judged by the respective B_{max} values (0.92 vs 0.16 a.u.).

The BDNF-MIP/SPE sensor showed a pseudo-linear response to the BDNF in the concentration range from 0.01 to 0.06 ng/mL and a fixed concentration of HSA (0.8 mg/mL), the main plasma protein (Fig. 7). The linear regression in this concentration range gives the coefficient of determination, *R*-squared, equal to 0.991 and LOD and LOQ values, determined as
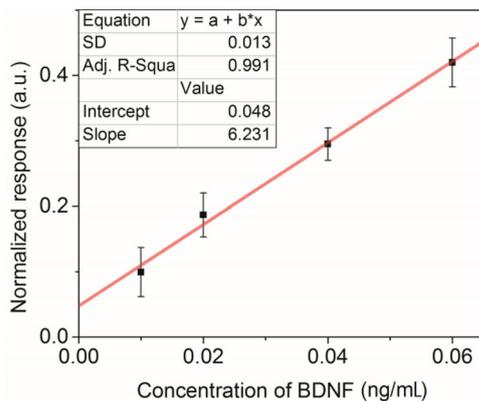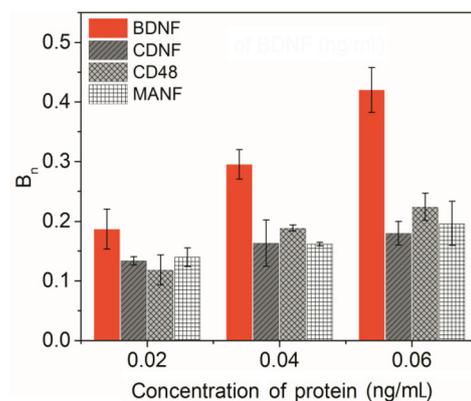
Fig. 7. Responses of the BDNF-MIP/SPE sensor at low concentrations of BDNF in the presence of 0.8 mg/mL HSA. The solid line represents the regression line.

Fig. 8. Selectivity test of the BDNF-MIP towards BDNF, CDNF, CD48, and MANF conducted through incubated in 0.02–0.06 ng/mL solutions of the respective proteins in PBS in the presence of 0.8 mg/mL HSA.

3 and 10 times the standard deviation (SD) divided by the slope of the regression line, 6 pg/mL and 20 pg/mL, respectively.

### 3.3. Selectivity and reusability study

The BDNF-MIP/SPE sensor was characterized in terms of its capability to rebind selectively the target protein, BDNF, with respect to the interfering proteins of slightly different size and isoelectric point (pI) such as CDNF, MANF, and mCD48. Selection of CDNF and MANF as interfering analytes was stipulated by their permanent presence in a human serum and thus, they can interfere with the sensor response along with the target protein (BDNF). The third interfering analyte – mCD48 – has the molecular weight and pI value similar to those of BDNF. The selectivity of the sensor was studied in the presence of HSA at a concentration of 0.8 mg/mL, corresponding to a 50-fold dilution of its physiological norm in diluted human serum. For the selectivity study, the concentration of the interfering proteins was selected close to their LOQ value (0.02–0.06 ng/mL). The response of the BDNF-MIP/SPE sensor to the BDNF was higher than that to the interfering proteins (Fig. 8). The difference between the responses of the sensor upon the interaction with the BDNF and the interfering proteins increased with the increasing concentration, and at 0.06 ng/mL the BDNF caused about a two times higher response as compared to the interfering proteins. At the same time the responses to the interfering proteins remained at approximately the same level for all tested concentrations.

As to the possibility of regenerating and repeatedly using a sensor, protein-MIP based sensors have been considered to have a significant advantage over conven-

tional antibody-based biosensors. Therefore, we examined the ability of the prepared BDNF-MIP/SPE sensor to withstand the regeneration procedure. The treatments in the acidic and alkaline solutions efficiently disrupting possible multiple hydrogen and electrostatic bonds between the protein and the MIP surface were assessed to regenerate the surface of the sensor. It was found that the response of the BDNF-MIP/SPE sensor was greatly reduced already after the first regeneration cycle (Fig. 9), indicating a poor reusability of the sensor. However, taking into account that a SPE-based sensor is expected to be used as a disposable sensor, its reusability is obviously not of great importance. On the other hand, comparison of the signals of three freshly prepared BDNF-MIP/SPEs showed that a good reproducibility of the sensor response (standard deviation 0.026) was achieved.
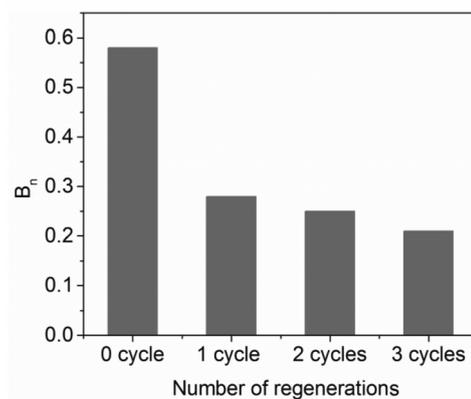
Fig. 9. Normalized responses of the BDNF-MIP/SPE sensor upon the injection of 2 ng/mL BDNF solution after 1, 2 and 3 regeneration cycles.

4. CONCLUSIONS

In the present study, we have developed for the first time a MIP synthetic receptor capable of selective binding of BDNF integrated with an inexpensive and disposable SPE. Surface-initiated C/LR photopolymerization was demonstrated to be a suitable method to prepare stable BDNF-MIP films directly on a SPE sensor. The prepared BDNF-MIPs were capable of binding BDNF with the dissociation constant, K_d, of 1.12 ng/mL and had about 5.8 times higher binding capacity than the reference film, NIP. The BDNF-MIP/SPE sensor could detect BDNF with the LOD value of 6 pg/mL and quantify BDNF with the LOQ value of 20 pg/mL in the presence of HSA as a highly abundant serum protein. Moreover, it was able to discriminate BDNF among analogous molecules, i.e. CDNF and MANF, and a molecule of a similar size, i.e. mCD48. Although further research is required, the presented approach to the preparation of a cost-effective MIP-SPE sensor capable of selective detection of a NF-family protein could be a promising route towards the development of innovative PoC diagnostics devices for the early-stage diagnostics of neurological diseases or for monitoring therapies.

ACKNOWLEDGEMENTS

REFERENCES

1. Larsson, A., Greig-Pylypczuk, R., and Huisman, A. The state of point-of-care testing: a European perspective. *Ups. J. Med. Sci.*, 2015, **120**, 1–10.
2. McMullan, J. T., Knight, W. A., Clark, J. F., Beyette, F. R., and Pancioli, A. Time-critical neurological emergencies: the unfulfilled role for point-of-care testing. *Int. J. Emer. Med.*, 2010, **3**, 127–131.
3. Wei, T-Y., Fu, Y., Chang, K-H., Lin, K-J., Lu, Y-J., and Cheng, C-M. Point-of-care devices using disease biomarkers to diagnose neurodegenerative disorders. *Trends Biotechnol.*, 2018, **36**, 290–303.
4. Piletsky, S. A. and Whitcombe, M. J. (eds). *Designing Receptors for the Next Generation of Biosensors*. Springer-Verlag, Berlin, 2013.
5. Mahon, C. S. and Fulton, D. A. Mimicking nature with synthetic macromolecules capable of recognition. *Nat. Chem.*, 2014, **6**, 665–672.
6. Mosbach, K. Molecular imprinting. *Trends Biochem. Sci.*, 1994, **19**, 9–14.
7. Tretjakov, A., Syritski, V., Reut, J., Boroznjak, R., and Öpik, A. Molecularly imprinted polymer film interfaced with Surface Acoustic Wave technology as a sensing platform for label-free protein detection. *Anal. Chim. Acta*, 2016, **902**, 182–188.
8. Cieplak, M. and Kutner, W. Artificial biosensors: How can molecular imprinting mimic biorecognition? *Trends Biotechnol.*, 2016, **34**, 922–941.
9. Haupt, K. and Mosbach, K. Molecularly imprinted polymers and their use in biomimetic sensors. *Chem. Rev.*, 2000, **100**, 2495–2504.
10. Ye, L. and Mosbach, K. Molecular imprinting: synthetic materials as substitutes for biological antibodies and receptors. *Chem. Mater.*, 2008, **20**, 859–868.
11. Espinoza-Castañeda, M., Escosura-Muñiz, A. d. l., Chamorro, A., Torres, C. d., and Merkoçi, A. Nano-channel array device operating through Prussian blue nanoparticles for sensitive label-free immunodetection of a cancer biomarker. *Biosens. Bioelectron.*, 2015, **67**, 107–114.
12. Tran, H. V., Piro, B., Reisberg, S., Huy Nguyen, L., Dung Nguyen, T., Duc, H. T., and Pham, M. C. An electrochemical ELISA-like immunosensor for miRNAs detection based on screen-printed gold electrodes modified with reduced graphene oxide and carbon nanotubes. *Biosens. Bioelectron.*, 2014, **62**, 25–30.
13. Tonello, S., Serpelloni, M., Lopomo, N. F., Sardini, E., Abate, G., and Uberti, D. L. (eds) *Preliminary Study of a Low-Cost Point-of-Care Testing System Using Screen-Printed Biosensors: For Early Biomarkers Detection Related to Alzheimer Disease*. IEEE International Symposium on Medical Measurements and Applications (MeMeA), 15–18 May 2016.
14. Lopes, F., Pacheco, J. G., Rebelo, P., and Delerue-Matos, C. Molecularly imprinted electrochemical sensor prepared on a screen printed carbon electrode for naloxone detection. *Sensor. Actuat. B-Chem.*, 2017, **243**, 745–752.
15. Ribeiro, J. A., Pereira, C. M., Silva, A. F., and Sales, M. G. F. Electrochemical detection of cardiac biomarker myoglobin using polyphenol as imprinted polymer receptor. *Anal. Chim. Acta*, 2017, **981**, 41–52.
16. WHO. *Neurological Disorders: Public Health Challenges*. World Health Organization, Geneva, Switzerland, 2006.
17. Cattaneo, A., Cattane, N., Begni, V., Pariante, C. M., and Riva, M. A. The human BDNF gene: peripheral gene expression and protein levels as biomarkers for psychiatric disorders. *Transl. Psych.*, 2016, **6**, e958.
18. Hashimoto, K. Brain-derived neurotrophic factor as a biomarker for mood disorders: an historical overview and future directions. *Psychiat. Clin. Neuros.*, 2010, **64**, 341–357.

19. Lindahl, M., Saarma, M., and Lindholm, P. Unconventional neurotrophic factors CDNF and MANF: structure, physiological functions and therapeutic potential. *Neurobiol. Dis.*, 2017, **97**, 90–102.

20. Lindholm, D., Mäkelä, J., Di Liberto, V., Mudò, G., Belluardo, N., Eriksson, O., and Saarma, M. Current disease modifying approaches to treat Parkinson's disease. *Cell. Mol. Life Sci.*, 2016, **73**, 1365–1379.

21. Laske, C., Stransky, E., Leyhe, T., Eschweiler, G. W., Wittorf, A., Richartz, E., et al. Stage-dependent BDNF serum concentrations in Alzheimer's disease. *J. Neural Transm.*, 2006, **113**, 1217–1224.

22. Sen, S., Duman, R., and Sanacora, G. Serum brain-derived neurotrophic factor, depression, and antidepressant medications: meta-analyses and implications. *Biol. Psychiat.*, 2008, **64**, 527–532.

23. Wang, Y., Liu, H., Zhang, B.-S., Soares, J. C., and Zhang, X. Y. Low BDNF is associated with cognitive impairments in patients with Parkinson's disease. *Parkinsonism Relat. D.*, 2016, **29**, 66–71.

24. Jolly, P., Tamboli, V., Harniman, R. L., Estrela, P., Allender, C. J., and Bowen, J. L. Aptamer–MIP hybrid receptor for highly sensitive electrochemical detection of prostate specific antigen. *Biosens. Bioelectron.*, 2016, **75**, 188–195.

25. Viswanathan, S., Rani, C., Ribeiro, S., and Delerue-Matos, C. Molecular imprinted nanoelectrodes for ultra sensitive detection of ovarian cancer marker. *Biosens. Bioelectron.*, 2012, **33**, 179–183.

26. Wang, Y. T., Zhang, Z. Q., Jain, V., Yi, J. J., Mueller, S., Sokolov, J., et al. Potentiometric sensors based on surface molecular imprinting: detection of cancer biomarkers and viruses. *Sensor. Actuat. B-Chem.*, 2010, **146**, 381–387.

27. Moreira, F. T. C., Sharma, S., Dutra, R. A. F., Noronha, J. P. C., Cass, A. E. G., and Sales, M. G. F. Protein-responsive polymers for point-of-care detection of cardiac biomarker. *Sensor. Actuat. B-Chem.*, 2014, **196**, 123–132.

28. Shumyantseva, V. V., Bulko, T. V., Sigolaeva, L. V., Kuzikov, A. V., and Archakov, A. I. Electrosynthesis and binding properties of molecularly imprinted poly-o-phenylenediamine for selective recognition and direct electrochemical detection of myoglobin. *Biosens. Bioelectron.*, 2016, **86**, 330–336.

29. Silva, B. V. M., Rodriguez, B. A. G., Sales, G. F., Sotomayor, M. D. T., and Dutra, R. F. An ultra-sensitive human cardiac troponin T graphene screen-printed electrode based on electropolymerized-molecularly imprinted conducting polymer. *Biosens. Bioelectron.*, 2016, **77**, 978–985.

30. Urraca, J. L., Aureliano, C. S. A., Schillinger, E., Esselmann, H., Wiltfang, J., and Sellergren, B. Polymeric complements to the Alzheimer's disease biomarker β-amyloid isoforms Aβ1–40 and Aβ1–42 for blood serum analysis under denaturing conditions. *J. Am. Chem. Soc.*, 2011, **133**, 9220–9223.

31. Cecchini, A., Raffa, V., Canfarotta, F., Signore, G., Piletsky, S., MacDonald, M. P., and Cuschieri, A. In vivo recognition of human vascular endothelial growth factor by molecularly imprinted polymers. *Nano Lett.*, 2017, **17**, 2307–2312.

32. Kamon, Y. and Takeuchi, T. Molecularly imprinted nanocavities capable of ligand-binding domain and size/shape recognition for selective discrimination of vascular endothelial growth factor isoforms. *ACS Sensors*, 2018, **3**, 580–586.

33. Johari-Ahar, M., Karami, P., Ghanei, M., Afkhami, A., and Bagheri, H. Development of a molecularly imprinted polymer tailored on disposable screen-printed electrodes for dual detection of EGFR and VEGF using nano-liposomal amplification strategy. *Biosens. Bioelectron.*, 2018, **107**, 26–33.

34. Salian, V. D., White, C. J., and Byrne, M. E. Molecularly imprinted polymers via living radical polymerization: relating increased structural homogeneity to improved template binding parameters. *React. Funct. Polym.*, 2014, **78**, 38–46.

35. Kidakova, A., Reut, J., Rappich, J., Öpik, A., and Syritski, V. Preparation of a surface-grafted protein-selective polymer film by combined use of controlled/living radical photopolymerization and micro-contact imprinting. *React. Funct. Polym.*, 2018, **125**, 47–56.

36. De Boer, B., Simon, H. K., Werts, M. P. L., Vegte, E. W. van der, and Hadziioannou, G. "Living" free radical photopolymerization initiated from surface-grafted iniferter monolayers. *Macromolecules*, 2000, **33**, 349–356.

37. Ahmad, R., Mocaer, A., Gam-Derouich, S., Lamouri, A., Lecoq, H., Decorse, P., et al. Grafting of polymeric platforms on gold by combining the diazonium salt chemistry and the photoiniferter method. *Polymer*, 2015, **57**, 12–20.

38. Roy, A., Gao, J., Bilbrey, J. A., Huddleston, N. E., and Locklin, J. Rapid electrochemical reduction of Ni(II) generates reactive monolayers for conjugated polymer brushes in one step. *Langmuir*, 2014, **30**, 10465–10470.

39. Pinson, J. and Podvorica, F. Attachment of organic layers to conductive or semiconductive surfaces by reduction of diazonium salts. *Chem. Soc. Rev.*, 2005, **34**, 429–439.

40. Anothumakkool, B., Guyomard, D., Gaubicher, J., and Madec, L. Interest of molecular functionalization for electrochemical storage. *Nano Res.*, 2017, **10**, 4175–4200.

41. Jian, W., Firestone, M. A., Auciello, O., and Carlisle, J. A. Surface functionalization of ultra-nanocrystalline diamond films by electrochemical reduction of aryldiazonium salts. *Langmuir*, 2004, **20**, 11450–11456.

42. Verheyen, E., Schillemans, J. P., van Wijk, M., Demeniex, M. A., Hennink, W. E., and van Nostrum, C. F. Challenges for the effective molecular imprinting of proteins. *Biomaterials*, 2011, **32**, 3008–3020.

Sensormaterjalid molekulaarselt jäljendatud polümeeridest patsiendimanusteks testideks

Anna Kidakova, Jekaterina Reut, Roman Boroznjak, Andres Öpik ja Vitali Syritski

Kliinilises diagnostikas on pidevalt kasvav vajadus kiirete, suure tundlikkuse ja selektiivsusega usaldusväärsete analüüsimeetodite järele, mis samal ajal on odavad, portatiivsed ning mugavad analüüside läbiviimiseks vahetult sündmuskohal (*point-of-care* (PoC)). PoC-testidele esitatavaid nõudeid võivad edukalt täita sensorid, mis põhinevad sünteetilistel retseptoritel molekulaarselt jäljendatud polümeeride (MIP) baasil ja mis erinevalt looduslikest retseptoritest on odavamad ning stabiilsemad. Antud töös on esmakordselt välja töötatud kliiniliselt olulise valgu neurotrofiini BDNF suhtes selektiivne MIP-retseptor ja ühendatud odava elektrokeemilise sensorplatvormiga SPE (*screen-printed electrode*). BDNF-MIP-kiled valmistati SPE pinnal "elava" radikaal-fotopolümerisatsiooni meetodil. Valmistatud BDNF-MIP/SPE elektrokeemiline sensor oli võimeline tuvastama BDNF-i konkureeriva HSA-valgu foonil avastamispiiriga 6 pg/mL ja eristama BDNF-molekuli selle struktuursetest analoogidest CDNF ning MANF. Väljapakutud meetod neurotrofiini BDNF suhtes selektiivse sensori valmistamiseks osutub perspektiivseks lahenduseks uute patsiendimanuste testide (PoC-testid) väljatöötamisel neuroloogiliste haiguste diagnostikaks ja/või ravi edukuse jälgimiseks.